Exact solutions and infinite-order phase transitions for a general class of Ising models on the regularized Apollonian network

J. Stat. Mech. (2014) P01010

(http://iopscience.iop.org/1742-5468/2014/1/P01010)

Journal of Statistical Mechanics: Theory and Experiment
An IOP and SISSA journal

Exact solutions and infinite-order phase transitions for a general class of Ising models on the regularized Apollonian network

M Serva[1,2], U L Fulco[1] and E L Albuquerque[1]

[1] Departamento de Biofísica e Farmacologia, Universidade Federal do Rio Grande do Norte, 59072-970 Natal-RN, Brazil
[2] Dipartimento di Ingegneria e Scienze dell'Informazione e Matematica, Università dell'Aquila, I-67010 L'Aquila, Italy
E-mail: serva@univaq.it, umbertofulco@gmail.com and eudenilson@gmail.com

Received 4 November 2013
Accepted for publication 8 December 2013
Published 17 January 2014

Online at stacks.iop.org/JSTAT/2014/P01010
doi:10.1088/1742-5468/2014/01/P01010

Abstract. The regularized Apollonian network (RAN) is defined starting from a tetrahedral structure with four nodes all connected. At any successive generations, new nodes are added and connected with the surrounding three nodes. As a result, a power-law cumulative distribution of connectivity $P(k) \propto 1/k^{\eta}$ with $\eta = \ln(3)/\ln(2) \simeq 1.585$ is obtained. We consider a very general class of Ising models on this network, whose exact solutions for both finite and infinite (thermodynamic limit) size are achieved by using an approach based on recursive partial tracing of the Boltzmann factor as an intermediate step for the calculation of the partition function. Afterwards, we focus on some relevant choices for the coupling constants between connected spins, and we show that ordinary ferromagnets and anti-ferromagnets (all equal couplings) do not undergo a phase transition. In contrast, some anti-ferrimagnets show an infinite-order transition, which is detected by the spontaneous magnetization M (and also by the coordination L, a second-order parameter), which, at transition, goes as $\exp[-b/(T_c - T)]$ for $T < T_c$, vanishing for $T > T_c$.

Keywords: rigorous results in statistical mechanics, classical phase transitions (theory), random graphs, networks

1742-5468/14/P01010+24$33.00

Contents

1. Introduction **2**

2. Regularized Apollonian network (RAN) **4**

3. Generalized Ising models on the RAN **6**

4. Exact solution of the general model **7**
4.1. Finite size 7
4.2. Thermodynamic limit 9

5. Exact solution of the Ising model with vanishing $h(n)$ and q **10**
5.1. Finite size 10
5.2. Thermodynamic limit 10

6. Simple cases **11**
6.1. Ordinary ferromagnet and anti-ferromagnet 11
6.2. A simple anti-ferrimagnet 12

7. Spontaneous magnetization and coordination **14**

8. The simple cases revisited **16**
8.1. Ordinary ferromagnet and anti-ferromagnet 16
8.2. The simple anti-ferrimagnet 17

9. Discussion **19**

Acknowledgments **20**

Appendix A **20**

Appendix B **21**

References **23**

1. Introduction

The regularized Apollonian network (RAN), as well as its original un-regularized version (the Apollonian one) [1], has a complex architecture characterized by a power-law distributed connectivity (scale free) and an average minimal path between two nodes smaller than any power of the system size (small-world effect) [1]. These two properties, which are shared by most real world networks, make Apollonian networks (ANs) intriguing substrates for statistical models of physical and biological phenomena, such as ideal Bose–Einstein condensation [2]–[6] or the transition from spreading to disappearance of an epidemic [7, 8], to cite just a few examples.

Classical statistical models on Apollonian networks have recently been the subject of many investigations, like the one proving that the democratic majority vote model displays

J. Stat. Mech. (2014) P01010

a second-order phase transition [9]. Ising models [10, 11] and the Potts model [12] have also been studied, and no critical properties have been detected, which is at variance with the results depicted in this paper where the presence of an infinite-order transition in some Ising models is discussed. This discrepancy is not striking since infinite-order transitions are elusive, it being difficult to show their presence either numerically or algebraically.

The Ising model on regular lattices usually undergoes a single second-order phase transition, as is well-known since the publication of the seminal exact solution of the two-dimensional ferromagnet by Onsager [13]. When the model on a regular lattice becomes very intricate with many phases [14], again only second-order phase transitions are observed, also when the substrate is a random network with exponentially distributed connectivity, as in the case of a diluted ferromagnet [15, 16], and even when it is a hierarchical fractal [17]–[19].

Nevertheless, infinite-order transitions have been sporadically observed in various models such as, for example, the two-dimensional F model of an anti-ferroelectric on a regular lattice [20], the Potts model of an anti-ferromagnet (only at the critical dimension) [21], and the Ising model of a ferromagnet on a random graph (at diverging critical temperature) [22].

An infinite-order transition has also been observed for the Ising model of a ferromagnet on a long-range inhomogeneous network [23]. In this paper the authors rigorously proved that in the absence of external magnetic field the free energy is a C^∞ function of the temperature at the critical point. This model was independently rediscovered fifteen years later, and solved stressing the differences from a Berezinskii–Kosterlitz–Thouless transition [24].

In this paper we consider a very general class of Ising models on the RAN characterized by the exchange coupling J_{ij} between spins on connected nodes, the local magnetic fields h_i, and by an interaction among triple spins. The couplings and the fields may have any kind of dependence on the connectivities of the involved nodes. Exact solutions are found for both finite and infinite (thermodynamic limit) network sizes. Our approach is based on recursive partial tracing of the Boltzmann factor as an intermediate step for the calculation of the partition function. We stress that our strategy works exactly for the Ising model on the RAN while, if applied to the un-regularized Apollonian network, it would only give approximate results. Our solution generalizes previous findings in [25] which were restricted to a few cases.

Afterwards, we focus our attention on some relevant choices for the coupling constants between spins on connected nodes, and we prove that ordinary ferromagnets and anti-ferromagnets (all equal couplings) do not undergo a phase transition. In contrast, some anti-ferrimagnets show a phase transition, which is detected by the spontaneous magnetization M and the coordination L (a second-order parameter). Both the magnetization M and the coordination L, at transition, go as $\exp[-b/(T_c - T)]$ for $T < T_c$, vanishing for $T > T_c$, so that they are C^∞ functions of the temperature at the critical point. Moreover, the free energy F and all its derivatives seem finite and continuous at T_c, so that the transition appears to be of infinite-order in spite of the presence of a spontaneous symmetry breaking.

The paper is organized as follows. In section 2 we describe the RAN model, together with its main properties. In section 3 we introduce the general class of Ising models,

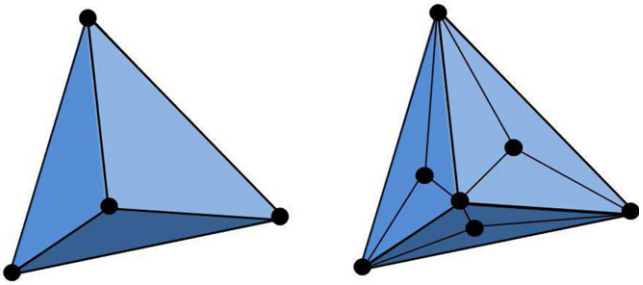

Figure 1. The RAN at generation $g = 0$ has four nodes all connected, forming a tetrahedral structure with six bonds (left picture). Each of the four triples of nodes individuates a different elementary triangle. At generation $g = 1$ a new node is added inside each of the four elementary triangles, and it is connected with the surrounding three nodes, so that the network has eight nodes, 18 bonds and 12 elementary triangles (right picture). The procedure is then iterated at any successive generation inserting new nodes in the last created elementary triangles, and connecting each of them with the three surrounding ones.

whose general solution is described in section 4 (leaving some lengthy calculations to appendix A). Then, some special cases are considered in section 5 (the magnetic field is absent but interactions are still generic) and in section 6 (restricted to the ordinary ferromagnetic and anti-ferromagnetic structures, for which we prove absence of transition, as well as to a simple anti-ferrimagnetic structure where a critical point seems to emerge). In order to confirm the criticality, we come back in section 7 to the general solution (non-vanishing magnetic field, generic couplings) depicting the temperature profiles of the spontaneous magnetization M and the coordination L (some lengthy calculations are left to appendix B). Then, in section 8, we restrict again our calculations to the ordinary ferromagnetic and anti-ferromagnetic structures, as well as to the simple anti-ferrimagnetic one in which, considering again the behavior of the two order parameters M and L, we show that indeed T_c is a critical point. Finally, a summary of our main achievements is presented in section 9.

2. Regularized Apollonian network (RAN)

The regularized Apollonian network (RAN) is defined starting from a $g = 0$ generation network with four nodes all connected, forming a tetrahedral structure with six bonds (see figure 1, left picture). Each of the four triples of nodes individuates a different elementary triangle. At generation $g = 1$ a new node is added inside each of the seven elementary triangles and it is connected with the surrounding three nodes, so that the network has eight nodes, 18 bonds and 12 elementary triangles (see figure 1, right picture). Then the procedure is iterated at any successive generation inserting new nodes in the last created elementary triangles, and connecting each of them with the three surrounding nodes. As a result, one has the following properties for a network of generation g:

- the number of new nodes created at any generation g' with $1 \leq g' \leq g$ is $V_{g'} = 4 \times 3^{g'-1}$;

- the total number of nodes at generation $g \geq 0$ is $N_g = 4 + \sum_{g'=1}^{g} 4 \times 3^{g'-1} = 2 \times 3^g + 2$;
- the number of new bonds created at any generation g' with $1 \leq g' \leq g$ is $4 \times 3^{g'}$;
- the total number of bonds at generation $g \geq 0$ is $U_g = 6 + \sum_{g'=1}^{g} 4 \times 3^{g'} = 2 \times 3^{g+1}$;
- the number of elementary triangles at generation $g \geq 0$ is 4×3^g.

Besides, we will use the following asymptotic relations which hold for large values of g: the total number of nodes is $N_g \simeq 2 \times 3^g$; the number of new nodes created at generation g is $V_g \simeq (2/3)\, N_g$; the total number of bonds is $U_g \simeq 3\, N_g$; the number of new bonds created at generation g is $\simeq (2/3)\, U_g \simeq 2\, N_g$.

The connectivity of a node is defined as the number of connections to other nodes. In the RAN the connectivity of each of the already existing nodes (so-called old nodes) is doubled when the generation is updated, while the connectivity of the newly created nodes (the new nodes) always equals 3, leading to the following relevant property.

- The connectivity at generation g of a node i only depends on its age. More explicitly, its connectivity is $3 \times 2^{g-g'_i}$, where g'_i is the generation at which it was created, and $n_i = g - g'_i$ is its age.

This property, which is crucial for our exact solution via renormalization, is not shared by the AN. In fact, in the AN the connectivity depends on both age and geometry since the three nodes at the three external corners have a variant connectivity. Moreover, in the RAN:

- any bond is shared by two elementary triangles,

which is also crucial for our exact solution and does not hold for the AN. In fact, in the AN the bonds connecting two of three external corners only have a single adjacent elementary triangle.

Finally, the following property, which we will use for defining our general class of Ising models, also holds:

- the age n_{ij} of a bond connecting nodes i and j is the same as the age of the younger of the two connected nodes, i.e. $n_{ij} = \min\{n_i, n_j\}$,

where n_i, n_j are only determined by the connectivities k_i and k_j, i.e. $k_i = 3 \times 2^{n_i}$, $k_j = 3 \times 2^{n_j}$.

In order to complete the characterization of the RAN, let us also describe the connectivity distribution:

- the number of nodes having connectivity k is $m(k, g)$, which equals $4 \times 3^{g-g'-1}$ if $k = 3 \times 2^{g'}$ with $g' = 0, \ldots, g-1$, equals 4 if $k = 3 \times 2^g$, and equals 0 otherwise.

Accordingly, the cumulative distribution of connectivity $P(k)$ is

- $P(k) = \sum_{r' \geq k} m(k', g)/N_g$, which, for large values of g, exhibits a power-law behavior, i.e., $P(k) \propto 1/k^\eta$, with $\eta = \ln(3)/\ln(2) \simeq 1.585$,

while the average connectivity can be simply computed as $2U_g/N_g \simeq 6$, where the approximate equality holds for large g.

The power-law cumulative distribution of connectivity $P(k)$ is shared with the AN as well. Analogously to the AN, the RAN is scale free and, as already mentioned, it displays the small-world effect. Finally, since the RAN can be constructed by four ANs (the four faces of the RAN tetrahedral structure), forcing the corner nodes to coincide, the thermodynamics of the two models, AN and RAN, are the same.

We stress once more that the reason for regularizing the AN is that in the RAN, at variance with the AN, the connectivity of the nodes only depends on their age and all bonds share two elementary triangles. The removal of the asymmetry associated with the corners allows for exact iterative calculations; in the AN they can be performed only approximatively.

3. Generalized Ising models on the RAN

We consider generalized Ising models defined according to the following Hamiltonian:

$$H_g = -\sum_{i,j} J_{ij}\sigma_i\sigma_j - \sum_i h_i\sigma_i - q\sum_{i,j,l}\sigma_i\sigma_j\sigma_l, \tag{3.1}$$

where the first sum goes on all U_g connected pairs of nodes of the RAN of generation g, the second sum goes on all N_g nodes, and the third one only goes on the 4×3^g elementary triangles of the last generation g (one of the nodes i, j or k is lastly created). The auxiliary variable q is introduced only for technical reasons which will become clear later, the relevant physics corresponding to $q \to 0$.

The most general class of models which comply with the symmetry of the RAN is achieved assuming that the exchange coupling J_{ij} and the local fields h_i depend on the connectivities of the involved nodes. In other words, $J_{ij} = J(k_i, k_j)$ and $h_i = h(k_i)$. Since $k_i = 3\times 2^{n_i}$, where $n_i = g_i - g'_i$ is the age of node i, in the RAN, the connectivity dependence is the same as the age dependence. This implies that we can rewrite $J_{ij} = J(n_i, n_j)$ and $h_i = h(n_i)$.

Another very general class can be achieved assuming that the exchange coupling J_{ij} depends on the age of the bond connecting nodes i and j and the local field h_i depends on the age of node i, i.e. $J_{ij} = J(n_{ij})$ and $h_i = h(n_i)$. Since $n_{ij} = \min\{n_i, n_j\}$, it is clear that this second class is contained in the first.

In this work we restrict ourselves to this second case so that, at generation g, the model is fully determined by the coupling values $J(0), J(1), \ldots, J(n), \ldots, J(g)$; the local field values $h(0), h(1), \ldots, h(n), \ldots, h(g)$; and the auxiliary variable value q. The integer argument $n = g - g'$ is either the age of the bonds or of the nodes; in particular, $n = 0$ corresponds to the last created bonds and nodes ($g = g'$), and $n = g$ to the bonds and nodes of the initial tetrahedral structure ($g' = 0$). It is useful to introduce the short notation $\mathbf{J} = \{J(0), J(1), \ldots, J(n), \ldots, J(\infty)\}$ and $\mathbf{h} = \{h(0), h(1), \ldots, h(n), \ldots, h(\infty)\}$, in such a way that a model of generation g is fully determined by the first $g + 1$ components of $\mathbf{J}$ and $\mathbf{h}$.

The couplings $J(n)$ can be all positive (ferrimagnet) or all negative (anti-ferrimagnet), or may have different signs (disordered). In particular, if all $J(n)$ are equal and positive,

the model is ordinary ferromagnetic; if they are all equal but negative, it is ordinary anti-ferromagnetic.

The partition function is

$$Z_g = \sum_{\#} \exp(-\beta H_g), \tag{3.2}$$

where the sum goes on all 2^{N_g} configurations. Here β is the inverse temperature, i.e., $\beta = 1/T$ (we consider a unitary Boltzmann constant k_{B}). The partition function $Z_g = Z_g(\beta, \mathbf{J}, \mathbf{h}, q)$ depends on β, q, and $J(0), J(1), \ldots, J(n), \ldots, J(g)$, $h(0), h(1), \ldots, h(n), \ldots, h(g)$ which are the first $g+1$ components of $\mathbf{J}$ and $\mathbf{h}$. The finite size free energy

$$F_g = -\frac{1}{\beta N_g} \log(Z_g) \tag{3.3}$$

depends on the same finite set of variables, i.e. $F_g = F_g(\beta, \mathbf{J}, \mathbf{h}, q)$. Finally, the thermodynamics can be obtained from the infinite size limit $g \to \infty$ (implying $N_g \to \infty$):

$$F(\beta, \mathbf{J}, \mathbf{h}, q) = \lim_{g\to\infty} F_g(\beta, \mathbf{J}, \mathbf{h}, q), \tag{3.4}$$

where now the dependence is on β, q, and all the infinite set of couplings $\mathbf{J} = \{J(0), J(1), \ldots, J(n), \ldots J(\infty)\}$ and fields $\mathbf{h} = \{h(0), h(1), \ldots, h(n), \ldots h(\infty)\}$.

Note that this limit is on the same grounds as the analogous limit for a one-dimensional Ising model, where the exchange couplings $J(d)$ depend on the distance $d = |i - j|$. In fact, on an open string of size N, the model depends on a finite number $J(1), J(2), \ldots, J(d), \ldots, J(N-1)$ of values, while in the thermodynamic limit this number becomes infinite.

Our strategy consists in performing a partial sum in (3.2) with respect to the $4 \times 3^{g-1}$ spin variables over nodes created at the last generation g. This sum generates new effective exchange couplings between all remaining spins, new local fields and a new auxiliary variable. In other words, we exactly map the g generation model in the same $g-1$ model with a new set of parameters $\mathbf{J}_1$, $\mathbf{h}_1$ and q_1, this technique working for any possible choice of the initial set $\mathbf{J}$, $\mathbf{h}$ and q. We stress that our approach is different when compared to the transfer matrix technique [10, 11], and it gives exact expressions for the thermodynamic variables in the $g \to \infty$ limit. Although we have a proof that confirms the absence of transition in the ordinary ferromagnetic and anti-ferromagnetic models, we are able to show the presence of an infinite-order phase transition in simple anti-ferrimagnetic models. The transition occurs at a finite temperature and, therefore, our result is at variance with previous findings [10, 11], where no critical behavior at a finite temperature was identified for this kind of model.

4. Exact solution of the general model

4.1. Finite size

The partial sum on spins over new nodes in (3.2) yields, after some lengthy but straightforward calculations (see appendix A), the following equality:

$$F_g(\beta, \mathbf{J}, \mathbf{h}, q) = \frac{N_{g-1}}{N_g} F_{g-1}(\beta, \mathbf{J}_1, \mathbf{h}_1, q_1) - \frac{V_g}{\beta N_g} A(\beta, J(0), h(0), q), \tag{4.1}$$

which derives directly from equation (A.11) of appendix A. Here $V_g = 4 \times 3^{g-1}$ is the number of spins on new nodes and $N_g = 2 \times 3^g + 2$ is the total number of spins. Moreover,

$$J_1(n) = J(n+1) + \frac{2}{\beta} B(\beta, J(0), h(0), q), \tag{4.2}$$

$$h_1(n) = h(n+1) + \frac{3 \times 2^n}{\beta} C(\beta, J(0), h(0), q), \tag{4.3}$$

and

$$q_1 = \frac{1}{\beta} D(\beta, J(0), h(0), q). \tag{4.4}$$

This equation gives the free energy $F_g(\beta, \mathbf{J}, \mathbf{h}, q)$ of a generation g model in terms of the free energy $F_{g-1}(\beta, \mathbf{J}_1, \mathbf{h}_1, q_1)$ of a generation $g-1$ model with new exchange couplings $J_1(n)$ and fields $h_1(n)$ (for both $0 \leq n \leq g-1$) and a new auxiliary variable q_1. All new parameters $\mathbf{J}_1, \mathbf{h}_1$, q_1 and the expression A which appear in (4.1) are explicit functions of the initial parameters $\mathbf{J}, \mathbf{h}$ and q. In appendix A we have calculated (derived from equations (A.4) to (A.7))

$$\begin{aligned} A(\beta, J, h, q) = {} & \tfrac{1}{8} \log[2^8 \cosh(\beta(3J + 3h + 3q)) \cosh(\beta(3J - 3h - 3q)) \\ & \times \cosh^3(\beta(J + 3h - q)) \cosh^3(\beta(J - 3h + q))], \end{aligned} \tag{4.5}$$

$$B(\beta, J, h, q) = \frac{1}{8} \log \left[\frac{\cosh(\beta(3J + 3h + 3q)) \cosh(\beta(3J - 3h - 3q))}{\cosh(\beta(J + 3h - q)) \cosh(\beta(J - 3h + q))} \right], \tag{4.6}$$

$$C(\beta, J, h, q) = \frac{1}{8} \log \left[\frac{\cosh(\beta(3J + 3h + 3q)) \cosh(\beta(J + 3h - q))}{\cosh(\beta(3J - 3h - 3q)) \cosh(\beta(J - 3h + q))} \right], \tag{4.7}$$

$$D(\beta, J, h, q) = \frac{1}{8} \log \left[\frac{\cosh(\beta(3J + 3h + 3q)) \cosh^3(\beta(J - 3h + q))}{\cosh(\beta(3J - 3h - 3q)) \cosh^3(\beta(J + 3h - q))} \right]. \tag{4.8}$$

Summarizing, we exactly map the g generation model with parameters $\mathbf{J}$, $\mathbf{h}$ and q in a $g-1$ model with a new set of parameters $\mathbf{J}_1$, $\mathbf{h}_1$ and q_1.

Relation (4.1) can be iterated, in order that the free energy of the generation $g-1$ is expressed in terms of the free energy of a generation $g-2$ model and so on. Thus

$$F_{g-r}(\beta, \mathbf{J}_r, \mathbf{h}_r, q_r) = \frac{N_{g-r-1}}{N_{g-r}} F_{g-r-1}(\beta, \mathbf{J}_{r+1}, \mathbf{h}_{r+1}, q_{r+1}) \tag{4.9}$$

$$- \frac{V_{g-r}}{\beta N_{g-r}} A(\beta, J_r(0), h_r(0), q_r), \tag{4.10}$$

where

$$J_{r+1}(n) = J_r(n+1) + \frac{2}{\beta} B(\beta, J_r(0), h_r(0), q_r), \tag{4.11}$$

$$h_{r+1}(n) = h_r(n+1) + \frac{3 \times 2^n}{\beta} C(\beta, J_r(0), h_r(0), q_r), \tag{4.12}$$

$$q_{r+1} = \frac{1}{\beta} D(\beta, J_r(0), h_r(0), q_r), \tag{4.13}$$

J. Stat. Mech. (2014) P01010

with $\mathbf{J}_0 = \mathbf{J}$, $\mathbf{h}_0 = \mathbf{h}$, $q_0 = q$. Note that at iteration r one has $0 \leq n \leq g - r$ so that the number of components $J(n)$ (or $h(n)$) to be computed is $g-r$, meaning that their number decreases by one at each iteration.

As a final result one has

$$F_g(\beta, \mathbf{J}, \mathbf{h}, q) = \frac{N_0}{N_g} F_0(\beta, J_g(0), h_g(0), q_g) - \frac{V_g}{\beta N_g} \sum_{r=0}^{g-1} \frac{1}{3^r} A(\beta, J_r(0), h_r(0), q_r). \tag{4.14}$$

$A, J_r(0), h_r(0)$ and q_r are given by (4.5), (4.11), (4.12) and (4.13), while $F_0(\beta, J, h, q)$ is the free energy of the Ising model on the initial tetrahedral structure with $N_0 = 4$ spins and 6 coupling, i.e.

$$F_0(\beta, J_g(0), h_g(0), q_g) = -\frac{1}{\beta N_0} \log \left(\sum_{\#} \exp(-\beta H_g^0) \right), \tag{4.15}$$

where the sum is on the 2^4 configurations of 4 spins, and

$$H_g^0 = -J_g(0) \sum_{i,j} \sigma_i \sigma_j - h_g(0) \sum_i \sigma_i - q_g \sum_{i,j,l} \sigma_i \sigma_j \sigma_l \tag{4.16}$$

is the Hamiltonian of the Ising model forming a tetrahedral structure with four spins and six couplings. Therefore, the first sum in (4.16) goes on the six pairs, the second sum on the four spins, and the third one on the four triples.

In conclusion, the finite size model is solved by iterating g times the finite set of equations (4.11), (4.12) and (4.13) and by computing the sum in (4.15) with $2^4 = 16$ terms.

We will see that this solution takes a particularly simple form when the $J(n)$ and $h(n)$ depend on a few control parameters. In this case, in fact, the set of iterative equations can be transformed into equations for the control parameters and a final explicit expression can be found.

4.2. Thermodynamic limit

Taking the limit $g \to \infty$ of equation (4.1) we obtain

$$F(\beta, \mathbf{J}, \mathbf{h}, q) = \frac{1}{3} F(\beta, \mathbf{J}_1, \mathbf{h}_1, q_1) - \frac{2}{3\beta} A(\beta, J(0), h(0), q), \tag{4.17}$$

where we have used $\lim_{g\to\infty} N_{g-1}/N_g = 1/3$ and $\lim_{g\to\infty} V_g/N_g = 2/3$. Also, $F(\beta, \mathbf{J}, \mathbf{h}, q) = \lim_{g\to\infty} F(\beta, \mathbf{J}, \mathbf{h}, q)$ is the thermodynamic free energy.

Note that this equation exactly maps the thermodynamic free energy with parameters $\mathbf{J}$, $\mathbf{h}$ and q into the free energy with parameters $\mathbf{J}_1$, $\mathbf{h}_1$ and q_1.

By iteration of the above equation or directly taking the $g \to \infty$ limit of equation (4.14), we also obtain

$$F(\beta, \mathbf{J}, \mathbf{h}, q) = -\frac{2}{3\beta} \sum_{r=0}^{\infty} \frac{1}{3^r} A(\beta, J_r(0), h_r(0), q_r), \tag{4.18}$$

where $J_r(0), h_r(0)$ and q_r are still given by equations (4.11), (4.12) and (4.13).

5. Exact solution of the Ising model with vanishing $h(n)$ and q

5.1. Finite size

In the case in which the local fields h_{ij} and the auxiliary variable are all vanishing, the solution is considerably simplified. In this case, in fact, not only $h(n) = 0$, $q = 0$ but it can easily verified from the relations depicted in the previous section that all $h_r(n)$ and all q_r vanish. The recursive relation becomes

$$F_{g-r}(\beta, \mathbf{J}_r) = \frac{N_{g-r-1}}{N_{g-r}} F_{g-r-1}(\beta, \mathbf{J}_{r+1}) - \frac{V_{g-r}}{\beta N_{g-r}} A(\beta J_r(0)), \tag{5.1}$$

where $\mathbf{J}_0 = \mathbf{J}$ and

$$J_{r+1}(n) = J_r(n+1) + \frac{1}{2\beta} \log[2\cosh(2\beta J_r(0)) - 1]. \tag{5.2}$$

Here A depends only on the product $\beta J_r(0)$ according to

$$A(\beta J_r(0)) = \frac{1}{4} \log[2\cosh(2\beta J_r(0)) - 1] + \log[2\cosh(\beta J_r(0))]. \tag{5.3}$$

By iteration, we have as a final result

$$F_g(\beta, \mathbf{J}) = \frac{N_0}{N_g} F_0(\beta J_g(0)) - \frac{V_g}{\beta N_g} \sum_{r=0}^{g-1} \frac{1}{3^r} A(\beta J_r(0)), \tag{5.4}$$

where $F_0(\beta J_g(0))$, which depends only on the product $\beta J_g(0)$, is the free energy of the Ising model on the initial of the tetrahedral structures with $N_0 = 4$ spins and six couplings, i.e.

$$F_0(\beta J_g(0)) = -\frac{1}{\beta N_0} \log \left[\sum_{\#} \exp \left(\beta J_g(0) \sum_{i,j} \sigma_i \sigma_j \right) \right], \tag{5.5}$$

where the sum before the exponential term is on the 2^4 configurations of the four spins, and the sum in the exponential is on the six possible pairs formed by the four spins.

5.2. Thermodynamic limit

Taking the thermodynamic limit $g \to \infty$ one immediately obtains

$$F(\beta, \mathbf{J}_r) = \frac{1}{3} F(\beta, \mathbf{J}_{r+1}) - \frac{2}{3\beta} A(\beta J_r(0)). \tag{5.6}$$

By iteration,

$$F(\beta, \mathbf{J}) = \frac{2}{3} \sum_{r=0}^{\infty} \frac{1}{3^k} A(\beta J_r(0)), \tag{5.7}$$

where the $J_r(0)$ are still obtained by (5.2).

Again, when the $J(n)$ depends on a few control parameters, the iterative equations (5.2) can be transformed into equations for the control parameters, and a final explicit expression can be found, as is shown in section 6.

6. Simple cases

6.1. Ordinary ferromagnet and anti-ferromagnet

In order to illustrate our strategy, we start with the simplest case in which all exchange interactions $J_{ij} = J$, $q = 0$ and all $h_i = 0$. The finite size free energy is

$$F_g(\beta J) = -\frac{1}{\beta N_g} \log \left[\sum_{\#} \exp \left(\beta J \sum_{i,j} \sigma_i \sigma_j \right) \right], \tag{6.1}$$

where the sum before the exponential term is on the 2^{N_g} configurations of the N_g spins, and the sum inside the exponential goes on the connected pairs of spins. Notice that $F_g(\beta J)$ only depends on the product βJ.

All $J_{ij} = J$ implies all $J(n) = J$, all $h_i = 0$ implies all $h(n) = 0$. Considering equation (5.2), it turns out that all $J_1(n) = J_1$. Therefore, in the thermodynamic limit,

$$F(\beta J) = \frac{1}{3} F(\beta J_1) - \frac{2}{3\beta} A(\beta J), \tag{6.2}$$

where

$$\beta J_1 = \beta J + \tfrac{1}{2} \log[2 \cosh(2\beta J) - 1], \tag{6.3}$$

and

$$A(\beta J) = \tfrac{1}{4} \log[2 \cosh(2\beta J) - 1] + \log[2 \cosh(\beta J)]. \tag{6.4}$$

The free energy is expressed in terms of the free energy of the same model with a different value J_1 for the exchange couplings. If J is positive (negative) the model is an ordinary ferromagnetic (anti-ferromagnetic). Since J_1 has the same sign as J, ferromagnetic (anti-ferromagnetic) is mapped into ferromagnetic (anti-ferromagnetic).

Note that the free energy of an ordinary ferromagnetic or anti-ferromagnetic model only depends on the product βJ. Therefore, if βJ is a transition point, the same occurs for βJ_1. In other words, (6.2) implies that if $F(\beta J)$ is non-analytical in a point βJ, it must be non-analytical in βJ_1 as well.

We can iterate the procedure

$$F(\beta J_r) = \frac{1}{3} F(\beta J_{r+1}) - \frac{2}{3\beta} A(\beta J_r), \tag{6.5}$$

and obtain, as a final result, the thermodynamic free energy in terms of a sum of explicit expressions:

$$F(\beta J) = \frac{2}{3} \sum_{r=0}^{\infty} \frac{1}{3^k} A(\beta J_r), \tag{6.6}$$

where

$$\beta J_r = \beta J_{r-1} + \tfrac{1}{2} \log[2 \cosh(2\beta J_{r-1}) - 1], \tag{6.7}$$

J. Stat. Mech. (2014) P01010

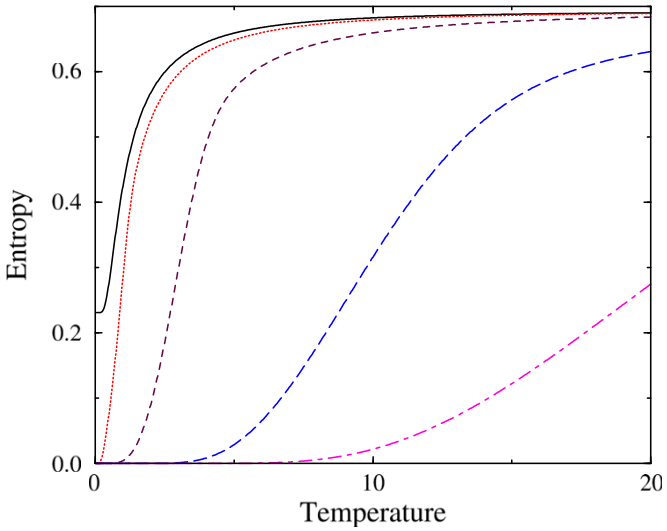

Figure 2. Entropy versus temperature T (in units of the Boltzmann constant k_B) for the following values of u (from the bottom): $u = 10, 5, 2, 1.2, 1$. The case $u = 1$ (full line) is the regular anti-ferromagnet with non-vanishing zero temperature entropy (entropy = $\log(2)/3$). This means that, due to frustration, there are about $2^{N_g/3}$ configurations of minimal energy. Interestingly, whenever $u > 1$, the zero temperature entropy drops to 0 since frustration is removed. In this case, in fact, the alignment of spins is determined by those couplings with a larger value, so that there are only two configurations of minimal energy.

with $J_0 = J$ and A given by (4.5). Note that both βJ_r and A only depend on βJ. If $J_0 = J$ is positive (ferromagnetism), the positive J_r increase monotonically and diverge for large r. On the other hand, if $J_0 = J$ is negative (anti-ferromagnetism) the negative J_r converge to 0 for large r. In both cases it is easy to verify that the sum (6.6) converges and there are not fixed points of the map (6.7) in the range $(0, \infty)$.

Since at any step of the iteration the initial model of parameter βJ is mapped into a new one of parameter βJ_r, a non-analytical point in βJ would imply an infinite number of non-analytical points βJ_r, proving the absence of transition.

The temperature profiles of the entropy and the specific heat for the anti-ferromagnetic structure ($J = -1$ without loss of generality) are depicted in figures 2 and 3, respectively. Notice that the zero temperature entropy is strictly positive.

6.2. A simple anti-ferrimagnet

Since we have proven that the constant coupling cases (ordinary ferromagnet and ordinary anti-ferromagnet) do not undergo a phase transition, we now extend our focus to consider a different model, now assuming that they can be different. Models with different values of the exchange couplings are usually denominated ferrimagnetic (or anti-ferrimagnetic). For ferrimagnetic models defined on a regular lattice, different exchange couplings usually correspond to different Euclidean distances of the connected nodes, while for models defined on hierarchical networks they may depend on the generation (as in the present model).

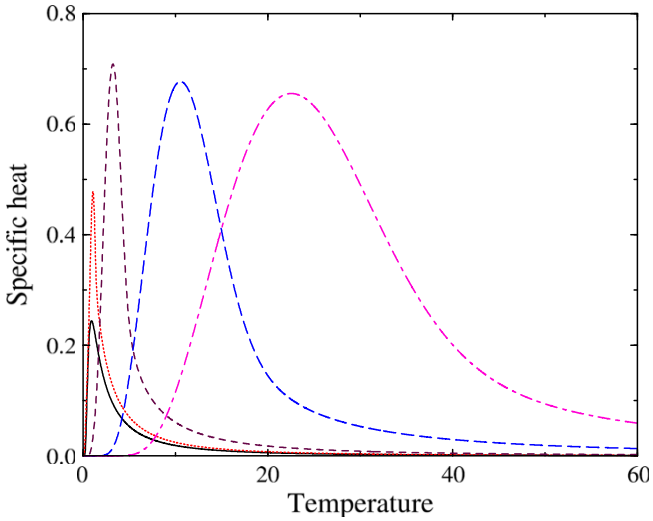

Figure 3. Specific heat versus temperature T (in units of the Boltzmann constant k_{B}) for the following values of u (from the right): $u = 10, 5, 2, 1.2, 1$. The curves, calculated in the thermodynamic limit $g \to \infty$, behave regularly and do not show any sign of phase transition. For example, in the case $u = 5$, one would expect a transition at $T = 49.16$ (see figure 4).

The simplest age dependence is $J_{i,j} = uJ$ for bonds of the last generation, and $J_{i,j} = J$ otherwise. In turn, this implies $J(0) = uJ$ and $J(n) = J$ for $n \geq 1$. If J is negative and u is non-negative, the model is anti-ferrimagnetic. Without loss of generality we can take $J = -1$ so that $J(0) = -u$ and $J(n) = -1$ for $n \geq 1$. The case $u = 1$ is the previously considered anti-ferromagnetic case, while an interesting phenomenology emerges for $u > 1$.

Then, following the same procedure as before, we take a partial sum with respect to the spins over the last created nodes, yielding the exact equality

$$F(\beta, \mathbf{J}) = \frac{1}{3} F(\beta J_1) - \frac{2}{3\beta} A(\beta u). \tag{6.8}$$

We stress that, while the initial anti-ferromagnet, described by $F(\beta, \mathbf{J})$, had two possible values for the couplings $\mathbf{J}$, namely $J(0) = -u$ and $J(n) = -1$ for $n \geq 1$, the effective model after the partial sum, described by $F(\beta J_1)$, has the single value J_1 for all components of $\mathbf{J}_1$. The new parameter J_1 and A can again be explicitly computed in terms of β and u,

$$A(\beta u) = \tfrac{1}{4} \log[2\cosh(2\beta u) - 1] + \log[2\cosh(\beta u)], \tag{6.9}$$

$$\beta J_1 = -\beta + \tfrac{1}{2} \log[2\cosh(2\beta u) - 1], \tag{6.10}$$

while the remaining J_r for $r \geq 2$ are again obtained by (6.7), and the free energy is given by (6.6). The resulting entropy and specific heat, as a function of the temperature T (in units of the Boltzmann constant k_{B}), are depicted in figures 2 and 3, respectively, for various values of u.

The case $u = 1$ is the regular anti-ferromagnet with non-vanishing zero temperature entropy (entropy $= \log(2)/3$). This means that, due to frustration, there are about $2^{N_g/3}$

configurations of minimal energy (the total number of possible configurations is 2^{N_g}). Interestingly, whenever $u > 1$, the zero temperature entropy drops to 0 since frustration is removed. In this case, in fact, the alignment of spins is determined by those couplings with a larger absolute value u, so that there are only two configurations of minimal energy (see figure 2).

Let us call β_c the (non-vanishing) value of β for which J_1 vanishes. Then, from (6.10), using $T_c = 1/\beta_c$, we have

$$T_c \log\left[2\cosh\left(\frac{2u}{T_c}\right) - 1\right] = 2. \tag{6.11}$$

The solution $T_c(u) = 1/\beta_c(u)$, which only depends on u, is shown in figure 4. Therefore, according to (6.10), we have the following.

(i) $\beta = \beta_c(u)$: in this case $J_1 = 0$ and one immediately obtains $F = (1/3)\log(2) + (1/6)\log[2\cosh(2u\beta_c(u)) - 1] + (2/3)\log[2\cosh(u\beta_c(u))]$.

(ii) $\beta > \beta_c(u)$: in this case $J_1 > 0$, i.e., the initial anti-ferrimagnet is mapped into an ordinary ferromagnet. The positive J_r increases monotonically and diverges for large r.

(iii) $\beta < \beta_c(u)$: in this case $J_1 < 0$, i.e., the initial anti-ferrimagnet is mapped into an ordinary anti-ferromagnet. The negative J_r converge monotonically to 0 for large r.

Is $T_c(u) = 1/\beta_c(u)$ a critical point? The answer to this question is not easy since all thermodynamic functions (all β derivatives of F) seem to be continuous at T_c including the specific heat (see figure 3). To address this question we study the behavior of some order parameter, as for example the spontaneous magnetization.

7. Spontaneous magnetization and coordination

Let us now return to the general Hamiltonian (3.1) and let us assume that the action of the external magnetic field h_i is proportional to the connectivity of the node, i.e.

$$h_i = p\, z_i, \tag{7.1}$$

where z_i is the connectivity of node i, implying $h(n) = 3 \times 2^n p$. We do not make assumptions on the exchange couplings J_{ij}, so that the $J(n)$ are left generic.

Accordingly, we can define the following spontaneous magnetization:

$$M(\beta, \mathbf{J}) = \lim_{g\to\infty} \frac{\sum_i z_i \langle\sigma_i\rangle}{\sum_i z_i} = -\frac{1}{6}\left[\frac{\partial F}{\partial p}\right]_{p=q=0^+}, \tag{7.2}$$

where we have used $\sum_i z_i = 2U_g \simeq 6N_g$. The notation $\langle\cdot\rangle$ indicates the average with respect to the Gibbs measure, in such a way that M satisfies $0 \le M \le 1$. The rationale for this choice is that it turns out to be the simplest tool in order to show the existence of an infinite-order phase transition in an anti-ferrimagnet.

J. Stat. Mech. (2014) P01010

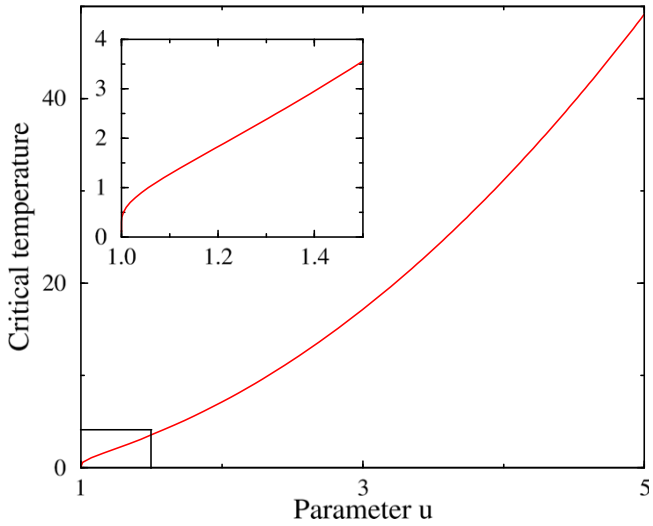

Figure 4. The critical temperature $T_c(u)$ computed as the non-vanishing solution of $T_c \log(2\cosh(2u/T_c)-1) = 2$. At $u = 1$ one has $T_c(u) = 0$ since this model is the ordinary anti-ferromagnet which, as we have proven, has no phase transition at a finite temperature. The inset shows that, indeed, $T_c(u)$ drops to 0 with diverging derivative when $u \to 1$. At $u = 5$ we have $T_c(u) = 49.16$, with no singularity depicted for the specific heat (see figure 3). Similar incongruence can be noticed for the other values of u considered in figure 3.

For the same practical reasons, we compute the *coordination*, a second-order parameter defined as

$$L(\beta, \mathbf{J}) = \lim_{g\to\infty} \frac{\sum_{i,j,k}\langle\sigma_i\sigma_j\sigma_j\rangle}{4\times 3^g} = -\frac{1}{2}\left[\frac{\partial F}{\partial q}\right]_{p=q=0^+}, \tag{7.3}$$

where the sum goes only on the 4×3^g triangles of the last generation g. Therefore, $\langle\sigma_i\sigma_j\sigma_k\rangle$ is the Gibbs average over a triple spin in triangles of the last generation g (one of the nodes i, j or k must be lastly generated).

Note that the factor $1/2$ in the last term comes from the fact that in the limit $g \to \infty$ one has $4 \times 3^g/N_g \to 2$, accordingly $|L| \leq 1$.

From appendix B we have

$$M(\beta, \mathbf{J}) = R_{11}M(\beta, \mathbf{J}_\infty) + R_{12}L(\beta, \mathbf{J}_\infty), \tag{7.4}$$

$$L(\beta, \mathbf{J}) = R_{21}M(\beta, \mathbf{J}_\infty) + R_{22}L(\beta, \mathbf{J}_\infty), \tag{7.5}$$

where R_{11}, R_{12}, R_{11} and R_{12} are the four elements of the 2×2 matrix $R(\beta, \mathbf{J})$ given by

$$R(\beta, \mathbf{J}) = \prod_{r=0}^{\infty} T(\beta J_r(0)). \tag{7.6}$$

Here, the 2×2 matrices $T(\beta J_r(0))$ have elements

$$T_{11}(\beta J_r(0)) = \tfrac{2}{3} + \tfrac{1}{4}[\tanh(3\beta J_r(0)) + \tanh(\beta J_r(0))], \tag{7.7}$$

$$T_{12}(\beta J_r(0)) = \tfrac{1}{12}[\tanh(3\beta J_r(0)) - 3\tanh(\beta J_r(0))], \tag{7.8}$$

$$T_{21}(\beta J_r(0)) = \tfrac{1}{4}[3\tanh(3\beta J_r(0)) - \tanh(\beta J_r(0))], \tag{7.9}$$

$$T_{22}(\beta J_r(0)) = \tfrac{1}{4}[\tanh(3\beta J_r(0)) + \tanh(\beta J_r(0))], \tag{7.10}$$

where the $J_r(0)$ are obtained from (5.2) with initial condition $J_0(n) = J(n)$. Besides, $M(\beta, \mathbf{J}_\infty)$ and $L(\beta, \mathbf{J}_\infty)$ are the magnetization and the coordination of the general Ising model with exchange coupling $\mathbf{J}_\infty$ and vanishing local fields and auxiliary variable. The exchange coupling $\mathbf{J}_\infty$ is the fixed point of the map (5.2).

8. The simple cases revisited

8.1. Ordinary ferromagnet and anti-ferromagnet

In the ordinary ferromagnetic case $J_0(n) = J > 0$ for all n, which implies that $J_r(n) = J_r > 0$ or all n and r. The value of J can be eventually taken equal to 1 without loss of generality.

Since the exchange couplings J_r depend only on the product βJ, and since $J_r(0) = J_r$, the matrix (7.6) depends only on βJ. Also, $M(\beta J)$ and $L(\beta J)$ only depend on βJ while $M(\beta J_\infty)$ and $L(\beta J_\infty)$ only depend on βJ_∞. Moreover, the end point J_∞ of the map (6.7) is infinite; therefore, $M(\beta J_\infty) = L(\beta J_\infty) = 1$ (ferromagnetism with an infinite value for the exchange couplings implies that all spins are aligned). Then, we can rewrite equations (7.4) and (7.5) as

$$M(\beta J) = R_{11}(\beta J) + R_{12}(\beta J), \qquad L((\beta J)) = R_{21}(\beta J) + R_{22}(\beta J), \tag{8.1}$$

where $R_{11}(\beta J)$, $R_{12}(\beta J)$, $R_{21}(\beta J)$ and $R_{22}(\beta J)$ are the elements of the 2×2 matrix R given by (7.6) with $J_r(0) = J_r$, and J_r given by (6.7) with initial condition $J_0 = J = 1$.

The matrix R can be easily computed and the resulting spontaneous magnetization and coordination are depicted in figure 5. As expected, both variables equal 1 at vanishing temperature because all spins are aligned, and they both decay to 0 when the temperature becomes infinite. Nevertheless, they are strictly positive at any finite temperature; otherwise a phase transition would be implied, which we have proven to be absent for this model.

In the ordinary anti-ferromagnetic case $J_0(n) = J < 0$ for all n, which implies that $J_r(n) = J_r < 0$ for all n and r. The value of J can be eventually taken equal to -1 without loss of generality. As we have seen, in this case J_r converges to 0 ($J_\infty = 0$) and, therefore, both $M(\beta, \mathbf{J}_\infty)$ and $L(\beta, \mathbf{J}_\infty)$ vanish. Equations (7.4) and (7.5) immediately imply

$$M(\beta, \mathbf{J}) = L(\beta, \mathbf{J}) = 0. \tag{8.2}$$

It can be easily verified that the matrix R vanishes as well, which would be enough by itself to ensure that both the spontaneous magnetization and the coordination vanish.

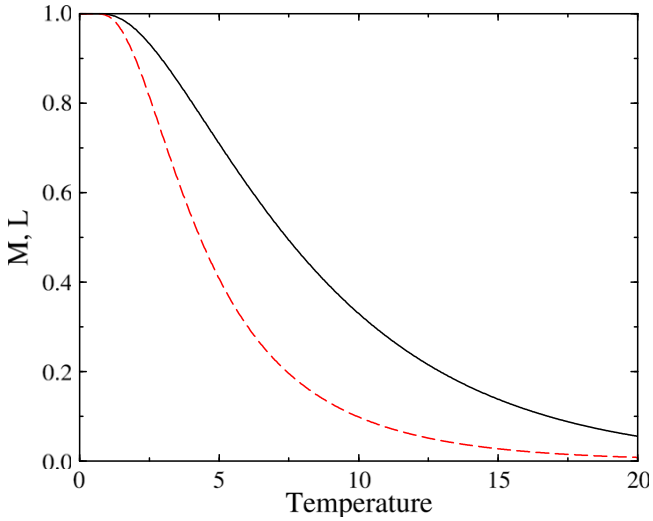

Figure 5. The spontaneous magnetization M (full line) and the coordination L (dashed line) versus the temperature T (in units of the Boltzmann constant k_{B}) for the ordinary ferromagnet. As expected, at vanishing temperature the system is fully ordered, with all spins pointing in the same direction, so that both the magnetization and the coordination are equal to 1. On increasing the temperature, both quantities decrease, vanishing at infinite temperature. Nevertheless, they are always strictly positive at finite temperature, since, as we have proven, transition is absent for this model.

8.2. The simple anti-ferrimagnet

In the anti-ferrimagnetic model $J_0(0) = -u < -1$ and $J_0(n) = -1$ for $n \geq 1$. If $T > T_{\mathrm{c}}$ the model u is mapped, after the first partial tracing, into an ordinary anti-ferromagnet. The sequence of J_r converges to 0 so that both $M(\beta, \mathbf{J}_\infty)$ and $L(\beta, \mathbf{J}_\infty)$ vanish. Moreover, analogously to the ordinary anti-ferromagnet, the matrix R vanishes as well. It is then straightforward to conclude that $M(\beta, \mathbf{J}) = L(\beta, \mathbf{J}) = 0$.

On the other hand, if $T < T_{\mathrm{c}}$ the model u is mapped, after the first partial tracing, into an ordinary ferromagnet. The sequence of J_r diverges (J_∞ is infinite) and, therefore, both $M(\beta, \mathbf{J}_\infty)$ and $L(\beta, \mathbf{J}_\infty)$ must equal one. However, it can be easily verified that the matrix R does not vanish so that both $M(\beta, \mathbf{J})$ and $L(\beta, \mathbf{J})$ are not vanishing. We have thus proven the existence of a transition at T_{c}.

The magnetization M and the coordination L for the $u = 5$ model are depicted in figure 6. From there one can notice that a negative coordination implies that the spins are preferentially organized, in order that in any elementary triangle one of them points in the opposite direction from the other two. This organization becomes exact at $T = 0$, where the coordination is -1. In this model, in fact, there is no frustration, since the alignment of spins is decided by the bonds with largest absolute value, i.e. the bonds with value $-u$ of the last generation. The triple of spins forming elementary triangles has two bonds with value $-u$ and one with value -1. Therefore, at vanishing temperature, there are always two spins pointing in the same direction, while the third one is pointing in the other direction, which implies $L = -1$.

doi:10.1088/1742-5468/2014/01/P01010

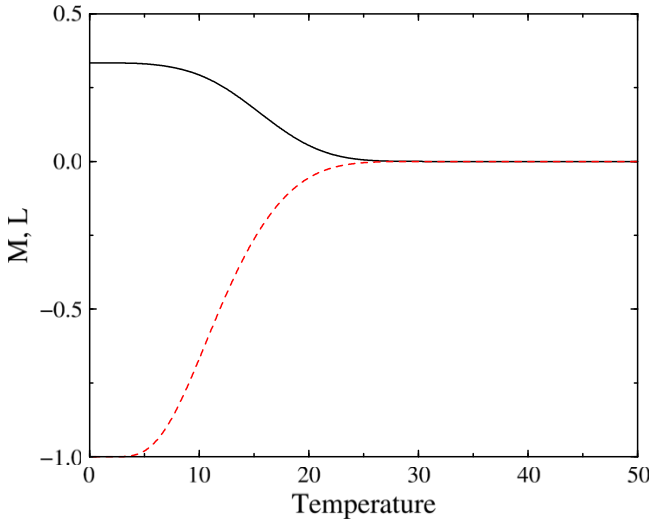

Figure 6. The spontaneous magnetization M (full line) and the coordination L (dashed line) versus the temperature T (in units of the Boltzmann constant k_{B}) for the $u = 5$ model. For both thermodynamic variables, it seems that transition occurs at a temperature around 26, while the expected transition temperature computed as the non-vanishing solution of $T_{\mathrm{c}} \log(2\cosh(2u/T_{\mathrm{c}}) - 1) = 2$ with $u = 5$ is $T_{\mathrm{c}} \simeq 49.16$. This difference is due to the wrong perception induced by the extra-slow decay to 0 of both variables (see figure 7). Indeed M and L are continuous with continuous derivatives of all orders in $T_{\mathrm{c}} \simeq 49.16$, where, nevertheless, they are non-analytical.

Observe also that the spontaneous magnetization M is positive below the critical temperature, with a value $1/3$ at $T = 0$. Absence of frustration implies that there are only two configurations of minimal energy. Since the alignment of spins is decided by the bonds with value $-u$, one has that all the lastly created V_g spins point in the same direction, while all the other $N_g - V_g$ spins point in the opposite direction. Therefore the magnetization is $[V_g - (N_g - V_g)]/N_g$, which, for large g (thermodynamic limit) equals $1/3$.

Then both variables M and L decay and vanish at the transition temperature. Apparently, the transition occurs at a temperature around 26, which is far from the transition temperature $T_{\mathrm{c}} \simeq 49.16$ obtained by the non-vanishing solution of $T_{\mathrm{c}} \log(2\cosh(2u/T_{\mathrm{c}}) - 1) = 2$ with $u = 5$. This is due to the fact that both M and L vanish extremely slowly. In order to make this evident, we have depicted $1/\log(M)$ and $1/\log(-L)$ in figure 7, which clearly show agreement with the expected critical temperature $T_{\mathrm{c}} \simeq 49.16$. The behavior of both the magnetization and the coordination, close to the critical point, is compatible with the function $\exp[-b/(T_{\mathrm{c}} - T)]$, which implies an infinite-order transition since M and L and all their derivatives are continuous at T_{c} as well the free energy and all its derivatives.

The phenomenology is qualitatively identical for all other values of $u > 1$. We can then summarized our result as follows.

(i) $T_{\mathrm{c}} \log(2\cosh(2u/T_{\mathrm{c}}) - 1) = 2$ individuates the transition temperature $T_{\mathrm{c}}(u)$.

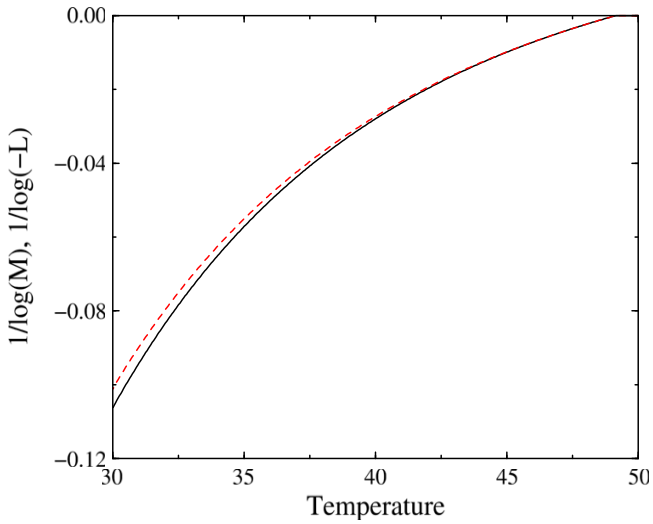

Figure 7. $1/\log(M)$ (full line) and $1/\log(-L)$ (dashed line) versus temperature T (in units of the Boltzmann constant k_B) for the $u = 5$ model. In figure 6 it seems that transition occurs at a temperature around 26, but this is a wrong perception. This figure shows indeed that the critical temperature (where both curves reach 0) is about $T_c = 49.16$, which is the correct transition temperature found as the non-vanishing solution of $T_c \log(2\cosh(2u/T_c) - 1) = 2$ with $u = 5$. This figure shows that the magnetization and the coordination, close to the critical point, go as $M \simeq L \sim \exp[-b/(T_c - T)]$, which implies that M and L are continuous with continuous derivatives of all orders in $T_c \simeq 49.16$ where, nevertheless, they are non-analytical.

(ii) The transition is of infinite-order with $M \simeq L \sim \exp[-b(u)/(T_c - T)]$ for T smaller but close to T_c, and $M = L = 0$ for T larger than T_c.

In the limit $u \to 1$ one can easily verify that $T_c = 0$ (see figure 4), confirming the absence of (positive temperature) transition in the ordinary anti-ferromagnet.

Our minimal choice $J_{i,j} = -u$ for newly created bonds, and $J_{i,j} = -1$ otherwise, is the simplest but not the only one which leads to an infinite-order phase transition. Indeed, there are many possible hierarchical choices for the $J_{i,j}$ which lead to the same qualitative behavior. The condition is anti-ferromagnetism with more recent bonds having a larger absolute value than older ones.

9. Discussion

The main results of this paper were:

(i) the exact solution for a general class of Ising models,

(ii) the infinite-order transition for a specific anti-ferrimagnet.

The first open problem that comes out from our results is how to classify all models which undergo the same phase transition, i.e. how to classify the possible choices of the

$J(n)$ that lead to a transition. For example, it is simple, using our strategy, to verify that the choice of all negative $J(n)$, with an absolute value decreasing with n and a non-vanishing $\lim_{n\to\infty} J(n)$, leads to a transition.

The anti-ferrimagnet discussed in the paper is in this class. Another simple example is $J(n) = -a - b/n^{\gamma}$ with positive a, b and γ. Nevertheless, it seems that the class is much more general, including many anti-ferrimagnetic models.

A second open problem is how to better characterize the transition. For example, at this stage we do not know the correlation function and we cannot comment about the relation with the Berezinskii–Kosterlitz–Thouless transition.

Finally, a mathematical problem remains open: to rigorously prove that the free energy is, indeed, C^{∞} at the transition point.

Acknowledgments

The authors would like to acknowledge the financial support from the Brazilian Research Agencies CAPES (Rede NanoBioTec and PNPD), CNPq (INCT-Nano(Bio) Simes, Casadinho-Procad) and FAPERN/CNPq (PRONEX). MS was partially supported by PRIN 2009 protocollo n. 2009TA2595.02.

Appendix A

Consider one of the nodes created at the last generation g and the three nodes which surround it. The contribution to $\exp(-\beta H_g)$ of this triangle is

$$\exp\left[\beta J\sigma_0(\sigma_1+\sigma_2+\sigma_3)+\beta 3h\sigma_0+\beta q\sigma_0(\sigma_1\sigma_2+\sigma_1\sigma_3+\sigma_2\sigma_3)\right], \tag{A.1}$$

where σ_0 is the spin in the center (new node) and σ_1, σ_2 and σ_3 are the spins at the three side nodes. The coupling J, the field h and q are those corresponding to the last created bonds, nodes and triangles, i.e., $J = J(0)$ and $h = h(0)$.

While σ_1, σ_2 and σ_3 also interact among themselves and with other spins, in neighboring triangles, σ_0 only interacts with these three surrounding ones. Therefore, its contribution can be traced out in an intermediate step for the computation of the partition function by taking the sum over the two possible values of σ_0 yielded by (A.1):

$$2\cosh\left[\beta J(\sigma_1+\sigma_2+\sigma_3)+\beta 3h+\beta q(\sigma_1\sigma_2+\sigma_1\sigma_3+\sigma_2\sigma_3)\right]. \tag{A.2}$$

The above expression is identical (i.e. it is equal for all 2^3 possible choices of the three spins σ_1, σ_2 and σ_3) to

$$\exp\left[A+B(\sigma_1\sigma_2+\sigma_1\sigma_3+\sigma_2\sigma_3)+C(\sigma_1+\sigma_2+\sigma_3)+D\sigma_1\sigma_2\sigma_3\right], \tag{A.3}$$

provided

$$\begin{aligned}\exp(8A) = 2^8 &\cosh[\beta(3J+3h+3q)]\cosh[\beta(3J-3h-3q)]\\ &\times \cosh^3[\beta(J+3h-q)]\cosh^3[\beta(J-3h+q)],\end{aligned} \tag{A.4}$$

$$\exp(8B) = \frac{\cosh[\beta(3J+3h+3q)]\,\cosh[\beta(3J-3h-3q)]}{\cosh[\beta(J+3h-q)]\,\cosh[\beta(J-3h+q)]}, \tag{A.5}$$

$$\exp(8C) = \frac{\cosh[\beta(3J+3h+3q)]\,\cosh[\beta(J+3h-q)]}{\cosh[\beta(3J-3h-3q)]\,\cosh[\beta(J-3h+q)]}, \tag{A.6}$$

$$\exp(8D) = \frac{\cosh[\beta(3J+3h+3q)]\,\cosh^3[\beta(J-3h+q)]}{\cosh[\beta(3J-3h-3q)]\,\cosh^3[\beta(J+3h-q)]}, \tag{A.7}$$

where it is intended that $J = J(0)$ and $h = h(0)$.

Partial trace over the $V_g = 4 \times 3^{g-1}$ new nodes created at generation g gives rise to an Ising model on the Apollonian network of generation $g-1$ where the new exchange coupling is

$$J_1(n) = J(n+1) + \frac{2}{\beta} B[J(0), h(0), q], \tag{A.8}$$

where $J(n+1)$ is the previous coupling (age is shifted from $n+1$ to n due to the fact that the last generation is eliminated). The last term is the extra exchange coupling coming from the partial tracing. The factor 2 in this last term comes from the fact that each of the bonds is shared by two triangles.

The new local field is

$$h_1(n) = h(n+1) + \frac{3 \times 2^n}{\beta} C[J(0), h(0), q]. \tag{A.9}$$

To understand the factor 3×2^n in the last term, consider that an old node of age $n+1$, before tracing, is connected to $z = 3 \times 2^{n+1}$ other nodes of which $z/2$ are new. Therefore, each old node receives from tracing a contribution C/β from the $z/2$ connected (and traced out) new nodes.

Finally, the new auxiliary variable is

$$q_1 = \frac{1}{\beta} D[J(0), h(0), q], \tag{A.10}$$

which connects only three spins in elementary triangles of generation $g-1$. We remark that a non-vanishing magnetic field $h(0)$ implies that $q_1 \neq 0$ even if $q = 0$, which is why, as a technical point, we had to include this variable from the beginning.

Furthermore, after partial trace, the partition function has a multiplicative extra term $\exp(V_g\, A)$, an extra term $\exp(A)$ for each of the new $V_g = 4 \times 3^{g-1}$ nodes. Therefore

$$Z_g(\beta, \mathbf{J}, \mathbf{h}, q) = Z_{g-1}(\beta, \mathbf{J}_1, \mathbf{h}_1, q_1) \exp\{V_g A(\beta, J(0), h(0), q)\}, \tag{A.11}$$

which immediately gives (4.1).

Appendix B

We assume $h_i = p\, z_i$, which implies $h(n) = 3 \times 2^n p$, while the couplings $J(n)$ are left generic. Given A and B in (A.4) and (A.5) with $J = J(0)$, $h = h(0) = 3p$ it turns out that

$$\left[\frac{\partial A}{\partial q}\right]_{p=q=0^+} = \left[\frac{\partial A}{\partial p}\right]_{p=q=0^+} = \left[\frac{\partial B}{\partial q}\right]_{p=q=0^+} = \left[\frac{\partial C}{\partial p}\right]_{p=q=0^+} = 0. \tag{B.1}$$

On the other hand, given C and D in (A.6) and (A.7) with $J = J(0)$, $h = h(0) = 3p$, we have

$$\left[\frac{\partial C}{\partial p}\right]_{p=q=0^+} = \frac{3\beta}{4}\Big[\tanh[3\beta J(0)] + \tanh[\beta J(0)]\Big], \tag{B.2}$$

$$\left[\frac{\partial C}{\partial q}\right]_{p=q=0^+} = \frac{\beta}{4}\Big[3\tanh[3\beta J(0)] - \tanh[\beta J(0)]\Big], \tag{B.3}$$

$$\left[\frac{\partial D}{\partial p}\right]_{p=q=0^+} = \frac{\beta}{4}\Big[3\tanh[3\beta J(0)] - 9\tanh[\beta J(0)]\Big], \tag{B.4}$$

$$\left[\frac{\partial D}{\partial q}\right]_{p=q=0^+} = \frac{3\beta}{4}\Big[\tanh[3\beta J(0)] + \tanh[\beta J(0)]\Big]. \tag{B.5}$$

Then, since $h(n) = 3 \times 2^n p$, equation (A.9) yields

$$h_1(n) = \frac{3 \times 2^n}{\beta}\Big[2p\beta + C(J(0), 3p, q)\Big], \tag{B.6}$$

which implies that the new local fields $h_1(n)$ have the same proportionality to the connectivity as the original $h(n)$, i.e. $h_1(n) \equiv 3 \times 2^n p_1$ with

$$p_1 \equiv 2p + \frac{1}{\beta}C(J(0), 3p, q). \tag{B.7}$$

This is the technical reason why we have considered from the beginning local fields with connectivity dependence $h_i + z_i p$.

According to (B.2) and (B.3) we have

$$T_{11}[\beta J(0)] = \frac{1}{3}\left[\frac{\partial p_1}{\partial p}\right]_{p=q=0^+} = \frac{2}{3} + \frac{1}{4}\Big[\tanh[3\beta J(0)] + \tanh[\beta J(0)]\Big], \tag{B.8}$$

$$T_{21}(\beta J(0)) = \left[\frac{\partial p_1}{\partial q}\right]_{p=q=0^+} = \frac{1}{4}\Big[3\tanh[3\beta J(0)] - \tanh[\beta J(0)]\Big]. \tag{B.9}$$

Using (B.4) and (B.5) together with (A.10) we have

$$T_{12}(\beta J(0)) = \frac{1}{9}\left[\frac{\partial q_1}{\partial p}\right]_{p=q=0^+} = \frac{1}{12}\Big[\tanh[3\beta J(0)] - 3\tanh[\beta J(0)]\Big], \tag{B.10}$$

$$T_{22}(\beta J(0)) = \frac{1}{3}\left[\frac{\partial q_1}{\partial q}\right]_{p=q=0^+} = \frac{1}{4}\Big[\tanh[3\beta J(0)] + \tanh[\beta J(0)]\Big], \tag{B.11}$$

which give all the necessary ingredients for the calculation of the magnetization and the coordination. From (4.17), (7.2) and (7.3)

$$M(\beta, \mathbf{J}) = T_{11}[\beta J(0)]M(\beta, \mathbf{J}_1) + T_{12}[\beta J(0)]L(\beta, \mathbf{J}_1), \tag{B.12}$$

$$L(\beta, \mathbf{J}) = T_{21}[\beta J(0)]M(\beta, \mathbf{J}_1) + T_{22}[\beta J(0)]L(\beta, \mathbf{J}_1). \tag{B.13}$$

Here,

$$M(\beta, \mathbf{J}_1) = -\frac{1}{6}\left[\frac{\partial F(\beta, \mathbf{J}_1, \mathbf{h}_1, q_1)}{\partial p_1}\right]_{p_1=q_1=0^+}, \tag{B.14}$$

$$L(\beta, \mathbf{J}_1) = -\frac{1}{2}\left[\frac{\partial F(\beta, \mathbf{J}_1, \mathbf{h}_1, q_1)}{\partial q_1}\right]_{p_1=q_1=0^+}, \tag{B.15}$$

are the magnetization and the coordination of the model with coupling $\mathbf{J}_1$ (we have used the fact that $p = q = 0^+$ implies $p_1 = q_1 = 0^+$).

The linear equations (B.12) and (B.13) can be iterated, yielding finally

$$M(\beta, \mathbf{J}) = R_{11} M(\beta, \mathbf{J}_\infty) + R_{12} L(\beta, \mathbf{J}_\infty), \tag{B.16}$$

$$L(\beta, \mathbf{J}) = R_{21} M(\beta, \mathbf{J}_\infty) + R_{22} L(\beta, \mathbf{J}_\infty), \tag{B.17}$$

where R_{11}, R_{12}, R_{21} and R_{22} are the four elements of the 2×2 matrix $R(\beta, \mathbf{J})$ given by

$$R(\beta, \mathbf{J}) = \prod_{r=0}^{\infty} T(\beta J_r(0)). \tag{B.18}$$

Also, $T[\beta J_r(0)]$ are 2×2 matrices whose elements are $T_{11}[\beta J_r(0)]$, $T_{12}[\beta J_r(0)]$, $T_{21}[\beta J_r(0)]$ and $T_{22}[\beta J_r(0)]$, while the $J_r(0)$ are given by (5.2), with $\mathbf{J}_0 = \mathbf{J}$.

We finally remark that $M(\beta, \mathbf{J}_\infty)$ and $L(\beta, \mathbf{J}_\infty)$ are the magnetization and the coordination of the general Ising model with vanishing local fields and auxiliary variable, whose exchange coupling $\mathbf{J}_\infty$ is the fixed point of the map (5.2).

References

[1] Andrade J S Jr, Herrmann H J, Andrade R F S and da Silva L R, *Apollonian networks: simultaneously scale-free, small world, Euclidean space filling with matching graphs*, 2005 *Phys. Rev. Lett.* **94** 018702

[2] Cardoso A L, Andrade R F S and Souza A M C, *Localization properties of a tight-binding electronic model on the Apollonian network*, 2008 *Phys. Rev.* B **78** 214202

[3] de Oliveira I N, de Moura F A B F, Lyra M L, Andrade J S Jr and Albuquerque E L, *Bose–Einstein condensation in the Apollonian complex network*, 2010 *Phys. Rev.* E **81** 030104(R)

[4] de Oliveira I N, de Moura F A B F, Caetano R A and Lyra M L, *Suppression of Bose–Einstein condensation in one-dimensional scale-free random potentials*, 2010 *Phys. Rev.* B **82** 172201

[5] de Oliveira I N, dos Santos T B, de Moura F A B F, Lyra M L and Serva M, *Critical behavior of the ideal-gas Bose–Einstein condensation in the Apollonian network*, 2013 *Phys. Rev.* E **88** 022139

[6] de Oliveira I N, de Moura F A B F, Lyra M L, Andrade J S Jr and Albuquerque E L, *Free-electron gas in the Apollonian network: multifractal energy spectrum its thermodynamic fingerprints*, 2009 *Phys. Rev.* E **79** 016104

[7] da Silva L F, Costa Filho R N, Soares D J B, Fulco U L and Albuquerque E L, *Critical properties of contact process on the Apollonian network*, 2013 *Physica* A **392** 1532

[8] da Silva L F, Costa Filho R N, Cunha A R, Macedo-Filho A, Serva M, Fulco U L and Albuquerque E L, *Critical properties of the SIS model dynamics on the Apollonian network*, 2013 *J. Stat. Mech.* P05003

[9] Lima F W S, Moreira A A and Araújo A D, *Nonequilibrium model on Apollonian networks*, 2012 *Phys. Rev.* E **86** 056109

[10] Andrade R F S and Herrmann H J, *Magnetic models on Apollonian networks*, 2005 *Phys. Rev.* E **71** 056131

[11] Andrade R F S, Andrade J S Jr and Herrmann H J, *Ising model on the Apollonian network with node-dependent interactions*, 2009 *Phys. Rev.* E **79** 036105

J. Stat. Mech. (2014) P01010

[12] Araújo N A M, Andrade R F S and Herrmann H J, *q-state Potts model on the Apollonian network*, 2010 *Phys. Rev.* E **82** 046109
[13] Onsager L, *A two-dimensional model with an order–disorder transition*, 1944 *Phys. Rev.* **86** 117
[14] Pasquini M and Serva M, *Two-dimensional frustrated Ising model with four phases*, 1997 *Phys. Rev.* E **56** 2751
[15] Serva M, *Magnetization densities as replica parameters: the dilute ferromagnet*, 2010 *Physica* A **389** 2700
[16] Serva M, *Exact approximate solutions for the dilute Ising model*, 2011 *Physica* A **390** 2443
[17] Bleher P M and Žalys E, *Asymptotics of the susceptibility for the Ising model on the hierarchical lattices*, 1989 *Commun. Math. Phys.* **120** 409
[18] Derrida B, De Seze L and Itzykson C, *Fractal structure of zeros in hierarchical models*, 1983 *J. Stat. Phys.* **33** 559
[19] Griffiths R B and Kaufman M, *Spin systems on hierarchical lattices. Introduction thermodynamic limit*, 1982 *Phys. Rev.* B **26** 5022
[20] Lieb E H, *Exact solution of the F model of antiferrolectric*, 1967 *Phys. Rev. Lett.* **18** 1046
[21] Berkert A N and Kadanoff L P, *Ground-state entropy algebraic order at low temperatures*, 1980 *J. Phys. A: Math. Gen.* **13** L259
[22] Dorogovtsev S N, Goltsev A V and Mendes J F F, *Ising model on networks with an arbitrary distribution of connections*, 2002 *Phys. Rev.* E **66** 016104
[23] Costin O, Costin R D and Griinfeld C P, *Infinite-order phase transition in a classical spin system*, 1990 *J. Stat. Phys.* **59** 1531
[24] Bauer M, Coulomb S and Dorogovtsev S N, *Phase transition with the Berezinskii–Kosterlitz–Thouless singularity in the Ising model on a growing network*, 2005 *Phys. Rev. Lett.* **94** 200602
[25] Serva M, Fulco U L and Albuquerque E L, *Ising models on the regularized Apollonian network*, 2013 *Phys. Rev.* E **88** 042823

J. Stat. Mech. (2014) P01010